

ORIGINAL ARTICLE

# Extracellular Matrix and Integrin Expression Profiles in Fuchs Endothelial Corneal Dystrophy Cells and Tissue Model

Benjamin Goyer, MSc,<sup>1,2,\*</sup> Mathieu Thériault, MSc,<sup>1,2,\*</sup> Sébastien P. Gendron, PhD,<sup>1,2</sup>  
Isabelle Brunette, MD, FRCSC,<sup>3,4</sup> Patrick J. Rochette, PhD,<sup>1,2,5</sup> and Stéphanie Proulx, PhD<sup>1,2,5</sup>

Primary corneal endothelial cell (CEC) cultures and 3D-engineered tissue models were used to study the aberrant deposition of extracellular matrix (ECM) in a vision impairing pathology known as Fuchs endothelial corneal dystrophy (FECD). CECs were isolated from excised Descemet membranes of patients with end-stage FECD. CECs isolated from healthy corneas served as controls. Microarray gene profiling was performed on postconfluent cultures of healthy and FECD cells. Protein expression analyses were conducted on tissue models that were engineered by seeding an endothelium on previously devitalized human stromal carriers. The engineered endothelia were kept in culture for 1–3 weeks to reform the endothelial monolayer. Protein expression of integrin subunits  $\alpha 4$ ,  $\alpha 6$ ,  $\alpha v$ , and  $\beta 1$ , as well as laminin, type IV collagen, fibronectin, clusterin, and transforming growth factor  $\beta$ -induced protein (TGF $\beta$ 1p) was then assessed by immunofluorescence. Microarray analysis showed nonstatistical twofold downregulation of collagen-coding genes (*COL4A4*, *COL8A2*, and *COL21A1*) and a twofold upregulation of the *COL6A1*, laminin  $\alpha 3$  gene *LAMA3*, and integrin subunit  $\alpha 10$  gene *ITGA10* in FECD cells. Fibronectin type III domain containing 4 (*FNDC4*) and integrin  $\beta 5$  (*ITGB5*) genes was significantly upregulated in FECD cells. Immunostainings demonstrated that the protein expression of the integrin subunits  $\alpha 4$ ,  $\alpha 6$ ,  $\alpha v$ , and  $\beta 1$ , type IV collagen, as well as laminin remained similar between native and engineered endothelia. TGF $\beta$ 1p expression was found on the stromal side of both FECD and healthy Descemet's membrane, and only one out of three FECD specimens was positive for the clusterin protein. Interestingly, the ECM protein fibronectin was also found to have a stronger presence on engineered FECD tissues, a result consistent with the native FECD specimens. To conclude, this study allowed to identify fibronectin deposition as one of the first steps in the pathogenesis of FECD, as defined by our engineered tissue model. This opens the way to an entirely new perspective for *in vitro* pharmacological testing of new therapies for FECD, the leading indication for corneal transplantation in North America.

**Keywords:** corneal endothelium, Fuchs corneal endothelial dystrophy, cell culture, tissue engineering, gene profiling, immunolocalization, extracellular matrix, integrins, fibronectin

## Introduction

**T**HE CORNEA IS the transparent tissue located in the front part of the eye. It is layered on its posterior surface by the corneal endothelium, which consists of a monolayer of confluent flattened cells responsible for maintaining corneal

transparency by ensuring constant stromal dehydration. Corneal endothelial cell (CEC) dysfunction results in corneal edema, loss of corneal transparency, and irreversible blindness.<sup>1</sup> Fuchs endothelial corneal dystrophy (FECD) is a slowly progressive corneal disease that becomes clinically evident in adults aged over 40. In 2015, FECD was

<sup>1</sup>Centre de Recherche du CHU de Québec–Université Laval, Axe Médecine Régénératrice, Hôpital du Saint-Sacrement, Québec, Canada.

<sup>2</sup>Centre de Recherche en Organogénèse Expérimentale de l'Université Laval/LOEX, Québec, Canada.

<sup>3</sup>Centre Universitaire d'Ophtalmologie de l'Université de Montréal et Centre de Recherche de l'Hôpital Maisonneuve-Rosemont, CIUSSS-E, Montréal, Canada.

<sup>4</sup>Hôpital Maisonneuve-Rosemont Research Center, CIUSSS-E, Montréal, Canada.

<sup>5</sup>Département d'Ophtalmologie et d'Oto-Rhino-Laryngologie–Chirurgie Cervico-Faciale, Faculté de Médecine, Université Laval, Québec, Canada.

\*These authors contributed equally to this work.

responsible for 15 707 (21.7%) of the 72 465 corneal transplantations performed in the United States.<sup>2</sup> There are currently no treatments for FECD other than corneal transplantation.

CECs secrete and deposit extracellular matrix (ECM) proteins that form a specialized basement membrane called Descemet's membrane (DM). A normal DM contains collagen type VIII, collagen type IV (chains  $\alpha 1$ – $\alpha 2$ ), and fibronectin on its stromal side and entactin, laminin, perlecan, and collagen type IV (chains  $\alpha 3$ – $\alpha 6$ ) on its endothelial side.<sup>3,4</sup> DM is composed of two layers, an anterior banded layer (fetal layer) of  $\sim 3 \mu\text{m}$  thickness that remains relatively constant after formation *in utero*, and a posterior nonbanded layer (postnatal) that is continuously produced during life. Its thickness reaches  $\sim 10 \mu\text{m}$  at age 80.<sup>5</sup>

The main feature of FECD is its irregular DM, which can be up to four times thicker than normal.<sup>6–8</sup> The anterior banded layer is normal, however, the posterior nonbanded layer is either absent or very thin. It is replaced by an abnormal collagenous banded layer that typically contains focal excrescences called guttae. In some cases, a loose fibrillar layer also embeds the guttae.<sup>6,9–11</sup> Previous reports showed an increased expression of collagen type IV, laminin, and fibronectin at the posterior side of the DM.<sup>12–14</sup> The glycoprotein clusterin and transforming growth factor  $\beta$ -induced protein (TGF $\beta$ Ip) have also been shown to be elevated in FECD and to colocalize at the guttae.<sup>14–16</sup> A recent study also reported an overexpression of the ECM proteins agrin, collagen type III, and collagen type XVI in the posterior collagenous layer of DM of FECD specimens.<sup>14</sup>

Integrins form a family of transmembrane glycoproteins that regulate cell–cell and cell–ECM interactions<sup>17,18</sup> They control many cellular processes, including adhesion, migration, proliferation, survival, and differentiation.<sup>19,20</sup> Integrins are heterodimeric molecules composed of an  $\alpha$  subunit, that confers most of the ECM ligand specificity, and a  $\beta$  subunit, that interacts with the intracellular cytoskeleton via adaptor proteins and determines the broad class of the receptor.<sup>21,22</sup> Eight  $\beta$ - and 18  $\alpha$ - subunits have been identified, that can associate with each other to produce the 24 integrin heterodimers reported to date.<sup>23–27</sup> Cultured healthy CECs were shown to express *ITGA1*, *ITGA2*, *ITGA3*, *ITGAV*, *ITGB1*, *ITGB3*, and *ITGB5* genes,<sup>28</sup> while native FECD endothelial cells were shown to upregulate *ITGA1*, *ITGA3*, *ITGA4*, *ITGAL*, *ITGB1*, *ITGB3*, and *ITGB4* genes.<sup>14</sup> To our knowledge, there has been no report on the integrin protein expression profile of the corneal endothelium, neither healthy nor diseased.

Reports on gene and protein expression in FECD describe the pathology at the end stage of the disease, since the specimens are obtained at the time of corneal transplantation or from postmortem tissues.<sup>14,29–31</sup> Knowing that DM thickening is the first clinical sign of the disease,<sup>32</sup> a better understanding of early ECM protein deposition could shed light on the pathogenesis of FECD. Recent advances in corneal tissue engineering bring us a unique opportunity to study early ECM deposition by FECD cells. Our group has reported on the successful culture of both normal<sup>33,34</sup> and FECD CECs.<sup>11</sup> We have used these cultured cells to engineer a corneal endothelium shown to be functional 1 week after transplantation in a living animal eye.<sup>35–37</sup> We now propose to use these novel engineered tissues to examine the

ECM protein deposition by the FECD cells and to characterize the integrin subunits that link these cells to a healthy DM. Understanding the aberrant deposition of ECM by the FECD cells may help to elucidate some of the aspects of FECD pathogenesis and lead to the development of new therapeutic approaches aimed at preventing abnormal ECM deposition and subsequent loss of endothelial cell functionality in this disease.

## Materials and Methods

### *Biological material*

This study was conducted according to our institutions' guidelines and the Declaration of Helsinki. Eighteen DM with attached endothelium were harvested from 18 consenting patients with end-stage clinical FECD at the time of their corneal transplantation<sup>11</sup> and were randomly assigned to one of the following groups. Six specimens were used for cell culture and gene expression profiling by microarray (age range: 58–82 years, mean  $\pm$  standard deviation [SD]:  $69 \pm 10$  years). Seven specimens were used to engineer corneal endothelia (age range: 58–77 years, mean  $\pm$  SD:  $67 \pm 8$  years). Five specimens were used for the immunostaining experiments (age range: 57–82 years, mean  $\pm$  SD:  $67 \pm 10$ ).

Native human corneas without endothelial diseases (healthy) and unsuitable for transplantation in human subjects were obtained from our local eye bank (Banque d'Yeux du Centre universitaire d'ophtalmologie [CUO], Québec, QC, Canada). These healthy corneas were used for cell culture and gene expression profiling by microarray (six corneas; age range: 58–82 years, mean  $\pm$  SD:  $71 \pm 10$  years), for the engineering of healthy corneal endothelia (two corneas; aged 47 and 68 years), as carriers for the engineered corneal endothelia (10 corneas; age range: 54–84 years, mean  $\pm$  SD:  $69 \pm 10$  years) and for the immunostaining experiments (seven corneas; range: 68–84 years, mean  $\pm$  SD:  $74 \pm 12$ ).

### *Isolation and culture of CECs from healthy and FECD corneas*

All CECs were isolated as described previously.<sup>38</sup> In brief, DM were peeled off and incubated overnight in growth medium at 37°C. After centrifugation, they were incubated 1 h in 0.02% ethylenediaminetetraacetic acid (Sigma, Oakville, ON, Canada), and the loosened cells were detached from the DM by passing several times through a flamed-polished pipet. Cells were then centrifuged and resuspended in fresh medium consisting of OptiMem-I (Invitrogen, Burlington, ON, Canada), 8% fetal bovine serum (HyClone, Logan, UT), 5 ng/mL human epidermal growth factor (Austral Biologicals, San Ramon, CA), 20 ng/mL nerve growth factor (Biomedical Technologies, Stoughton, MA), 100  $\mu\text{g}/\text{mL}$  bovine pituitary extract (Biomedical Technologies), 20  $\mu\text{g}/\text{mL}$  ascorbic acid (Sigma), 0.08% chondroitin sulfate (Sigma), 25  $\mu\text{g}/\text{mL}$  gentamicin sulfate (Scheringm Pointe Claire, QC, Canada), and 100 IU/mL penicillin G (Sigma). Cells were plated on dishes covered with a fibronectin, collagen, and albumin coating mix (FNC, Athena Enzyme Systems, Baltimore, MD).

### *Gene expression profiling*

Total RNA was isolated from postconfluent CEC cultures, as described.<sup>39</sup> Passage 2 or 3 cells were grown and cultured

for 24–38 days, with the addition of hydrocortisone (0.4  $\mu\text{g}/\text{mL}$ ) during the last 7 days of culture. Total RNA was isolated using the RNeasy Mini Kit (QIAGEN, Toronto, ON, CA) and RNA quality was analyzed using the 2100 Bioanalyzer (Agilent Technologies, Mississauga, ON, Canada). All samples had an RNA integrity number over 9.5. Cyanine 3-CTP labeled cRNA targets were prepared from 50 ng of total RNA, using the Agilent One-Color Micro-array-Based Gene Expression Analysis Kit (Agilent Technologies). The cRNA (600 ng) was incubated on a G4851A SurePrint G3 Human Gene Expression  $8 \times 60$  K array slide (60,000 probes, Agilent Technologies) and the slides were hybridized and scanned on an Agilent SureScan Scanner according to the manufacturer's instructions. The data were then analyzed using the ArrayStar V12 (DNASTAR, Madison, WI) software for scatter plots and for the generation of heat maps for selected genes of interest. The raw data generated from the arrays were also analyzed by RMA (Robust Multiarray Analysis) for background correction. It was subsequently transformed in  $\text{Log}_2$  base and quantile normalized before a linear model was fitted to the normalized data, to obtain an expression measure for each probe set on each array. The microarray data presented in this study complied with the minimum information about a microarray experiment requirements.<sup>40</sup>

#### Tissue-engineered human corneal endothelium

Eye bank corneas were devitalized using three freeze-thaw cycles,<sup>36</sup> then stored at  $-20^\circ\text{C}$  until used (range 17–620 days, mean  $\pm$  SD =  $88 \pm 106$  days). On the day of reconstruction, they were thawed, rinsed to remove the dead cells, and observed under a stereomicroscope (Nikon SMZ800, Mississauga, ON, Canada). Corneas with detached DM were discarded. Tissue engineering of the corneal endothelium followed our previously published protocol.<sup>36</sup> In brief, devitalized human corneas were placed in the bottom of a six-well plate, with the denuded DM facing up. Endothelial cells isolated from healthy ( $n=3$ ) and FECD ( $n=7$ ) corneas were seeded on top of the denuded DM and allowed to adhere for 4 h before immersion in culture medium. They were further cultured for 1–3 weeks (healthy CECs: from 9 to 16 days, mean  $\pm$  SD =  $11 \pm 2$  days; FECD CECs: from 8 to 20 days, mean  $\pm$  SD =  $13 \pm 3$  days). A flow diagram of the tissue engineering protocol is presented in Figure 1.

#### Histology

Tissues were fixed in 3.7% formaldehyde (ACP Chemicals, Montréal, QC, Canada) and processed for paraffin embedding. Sections (5  $\mu\text{m}$ ) were stained with Masson's trichrome. Digital images were acquired using an Axio Imager Z2 microscope (Carl Zeiss Canada Ltd., Toronto, ON, Canada).

#### Indirect immunofluorescence analysis

Tissues were embedded in Optimal Cutting Temperature compound (Somagen, Edmonton, AB, Canada), frozen in liquid nitrogen and stored at  $-80^\circ\text{C}$  for ulterior immunostaining. Indirect immunofluorescence assays were performed on 12  $\mu\text{m}$  cryosections as follows: for the clusterin/TGF $\beta$ 1p costaining, cryosections were fixed 10 min at  $-20^\circ\text{C}$  in methanol (100%; Commercial Alcohols, Brampton, ON,

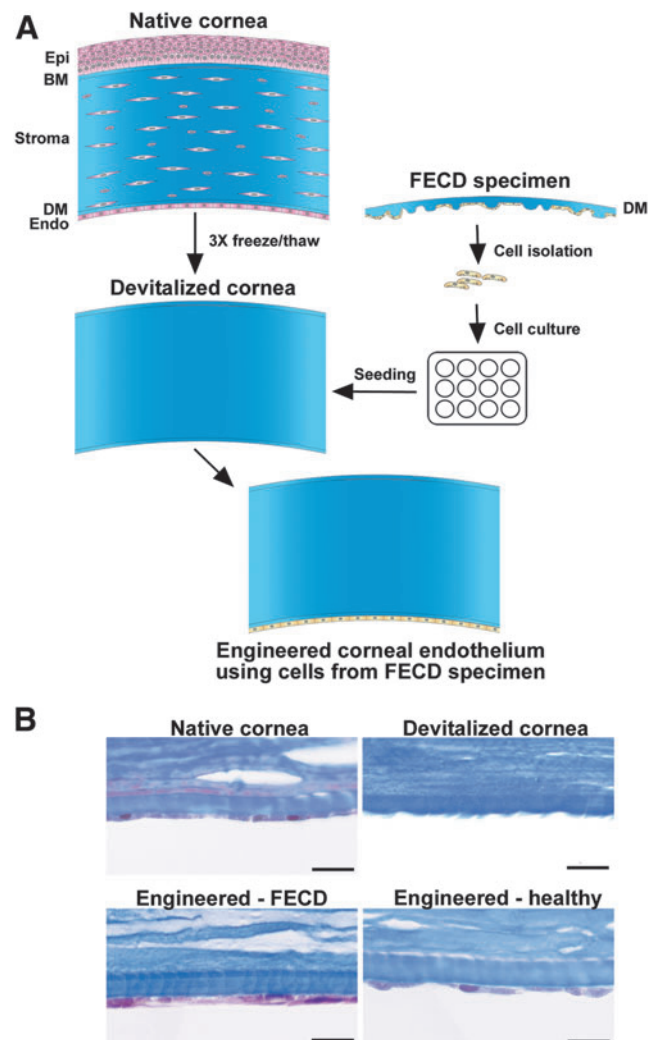


**FIG. 1.** Schematic representation of the tissue engineering protocol. **(A)** A healthy eye bank cornea was devitalized following three freeze-thaw cycles and used as a carrier for the engineering of a corneal endothelium using cultured cells isolated from FECD specimens. The same protocol was also used to engineer a corneal endothelium using healthy cells from normal eye bank corneas (not shown). **(B)** Histology cross-sections, trichrome Masson's staining. *Top left:* a native human eye bank cornea before devitalization; *Top right:* a devitalized human cornea before cell seeding. Note the absence of cells in the stroma and on Descemet's membrane; *Bottom left:* a corneal endothelium engineered using cells from patients with FECD; *Bottom right:* a corneal endothelium tissue engineered using healthy cells from an eye bank cornea. Scale bar: 20  $\mu\text{m}$ . FECD, Fuchs endothelial corneal dystrophy.

Canada), permeabilized with Triton-phosphate-buffered saline 1% (v/v) for 10 min and immunostained 2 h with a mouse anti-clusterin- $\alpha/\beta$  (H-330; Santa Cruz Biotechnology, Dallas, TX), and a goat anti-TGF $\beta$ 1p antibody (E-19; Santa Cruz Biotechnology). For all other immunostainings, cryosections were fixed 10 min at  $-20^\circ\text{C}$  with acetone (90%; EMD, Mississauga, ON, Canada) and immunostained with a rabbit anti-collagen IV (Abcam, Toronto, ON, Canada), a mouse anti-fibronectin (ATCC, Rockville, MD), a rat anti-laminin

TABLE 1. TRANSCRIPTOME ANALYSIS OF EXTRACELLULAR MATRIX-RELATED GENES IN FUCHS ENDOTHELIAL CORNEAL DYSTROPHY CULTURED CELLS

Gene name	Mean linear value $\pm$ SD	Fold change relative to healthy controls	p
<b>Collagen genes</b>			
<i>COL1A1</i>	823 $\pm$ 676	1.0	0.966
<i>COL1A2</i>	13 955 $\pm$ 5 286	-1.2	0.476
<i>COL3A1</i>	260 $\pm$ 130	-1.4	0.418
<i>COL4A1</i>	246 $\pm$ 374	-1.3	0.829
<i>COL4A2</i>	2 990 $\pm$ 3 582	-1.2	0.808
<i>COL4A3BP</i>	705 $\pm$ 128	1.1	0.236
<b><i>COL4A4</i></b>	298 $\pm$ 225	<b>-2.3</b>	0.329
<i>COL4A5</i>	1 630 $\pm$ 437	-1.1	0.591
<i>COL4A6</i>	2 043 $\pm$ 742	-1.2	0.311
<i>COL5A1</i>	361 $\pm$ 170	-1.3	0.471
<i>COL5A2</i>	5 303 $\pm$ 1 639	-1.2	0.451
<i>COL6A1</i>	7 333 $\pm$ 4 739	1.1	0.697
<b><i>COL6A2</i></b>	344 $\pm$ 524	<b>2.2</b>	0.426
<i>COL7A1</i>	526 $\pm$ 210	-1.4	0.132
<i>COL8A1</i>	11 144 $\pm$ 4 428	-1.7	0.052
<b><i>COL8A2</i></b>	823 $\pm$ 967	<b>-2.6</b>	0.146
<i>COL9A3</i>	2 178 $\pm$ 3 370	1.7	0.528
<i>COL12A1</i>	11 575 $\pm$ 6 420	-1.5	0.274
<i>COL13A1</i>	692 $\pm$ 362	1.4	0.376
<i>COL16A1</i>	1 580 $\pm$ 801	1.3	0.453
<i>COL18A1</i>	2 698 $\pm$ 1 685	1.2	0.648
<b><i>COL21A1</i></b>	98 $\pm$ 61	<b>-2.0</b>	0.206
<i>COL24A1</i>	119 $\pm$ 44	-1.5	0.306
<b>Fibronectin genes</b>			
<i>FNI</i>	1 402 $\pm$ 1 998	1.5	0.648
<i>FNDC3A</i>	140 $\pm$ 65	-1.2	0.532
<i>FNDC3B</i>	439 $\pm$ 131	1.1	0.751
<i>FNDC4</i>	350 $\pm$ 86	1.8	0.022 <sup>a</sup>
<b>Laminin genes</b>			
<b><i>LAMA3</i></b>	559 $\pm$ 796	<b>2.8</b>	0.313
<i>LAMA4</i>	318 $\pm$ 79	1.1	0.588
<i>LAMA5</i>	314 $\pm$ 70	1.1	0.454
<i>LAMB1</i>	360 $\pm$ 35	1.0	0.771
<i>LAMB2</i>	5 957 $\pm$ 1 634	-1.2	0.370
<i>LAMB3</i>	249 $\pm$ 176	1.9	0.163
<i>LAMC1</i>	1 589 $\pm$ 731	-1.1	0.660
<i>LAMC2</i>	238 $\pm$ 145	-1.2	0.713
<b>Other</b>			
<i>CLU</i>	6 668 $\pm$ 5 069	-1.3	0.508
<i>CLUAP1</i>	342 $\pm$ 80	-1.1	0.740
<i>TGFBI</i>	38 176 $\pm$ 5 415	1.3	0.105

Genes with linear values under 100 were excluded. Bold indicates a twofold down- or upregulation.

<sup>a</sup>Means significantly different ( $p < 0.05$ ).

FNDC4, fibronectin type III domain containing 4; SD, standard deviation.

(Abcam), a mouse anti-integrin  $\alpha 4$  (Millipore, Temecula, CA), a mouse anti-integrin  $\alpha 5$  (Transduction laboratories, Mississauga, ON, Canada), a mouse anti-integrin  $\alpha 6$  (Serotec, Burlington, ON, Canada), a rabbit anti-integrin  $\alpha v$  (Millipore), or a mouse anti-integrin  $\beta 1$  (ATCC) for 1 h at room temperature. Secondary antibodies consisted of a goat anti-rabbit, a goat anti-rat, a chicken anti-rabbit, a donkey anti-mouse conjugated with Alexa Fluor 594 (Life technologies, Burlington, ON, Canada) and a donkey anti-goat antibody con-

jugated with Alexa Fluor 647 (Abcam) for 1 h at room temperature. Negligible background was observed for controls (primary antibodies omitted). Cell nuclei were counterstained with Hoechst reagent 33258 (Sigma). Fluorescence was observed using a LSM700 confocal microscope (Zeiss, Toronto, ON, Canada).

#### Statistical analysis

Quantified data represent the mean  $\pm$  SD wherever applicable. Statistical significance was determined using the non-parametric Mann-Whitney U-test (GraphPad Prism version 5), which does not assume Gaussian distribution. A  $p < 0.05$  was considered significant.

## Results

### ECM- and integrin-related gene expression

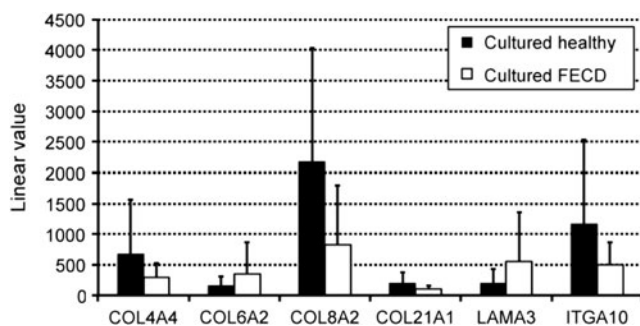
Gene expression profiling by microarray analysis was conducted on total RNAs isolated from cultured CECs from healthy and FECD specimens. Tables 1 and 2 summarize the ECM and integrin-related genes that had a mean linear value over 100. A high degree of variability was observed between samples (high SD values). Results show that 13% (5 out of 38) ECM-related genes and 6% (1 out of 18) integrin-related genes had a twofold change deregulation in FECD cells compared with healthy controls. The most abundant mRNAs (linear value over 10,000), in both FECD and healthy cultured CECs, were the ones expressed by *COL1A2*, *COL8A1*, *COL12A1*, and *TGFBI*. Mean linear values of genes with a twofold (or over) deregulation are represented in Figure 2. In FECD cells, downregulated genes included *COL4A4*, *COL8A2*, *COL21A1*, and *ITGA10*, while *COL6A2* and *LAMA3* were

TABLE 2. TRANSCRIPTOME ANALYSIS OF INTEGRIN-RELATED GENES IN FUCHS ENDOTHELIAL CORNEAL DYSTROPHY-CULTURED CELLS

Gene name	Mean linear value $\pm$ SD	Fold change relative to healthy controls	p
<b>Integrin genes</b>			
<i>ITGA1</i>	121 $\pm$ 51	-1.4	0.161
<i>ITGA3</i>	1 409 $\pm$ 439	1.0	0.843
<i>ITGA4</i>	336 $\pm$ 224	1.6	0.262
<i>ITGA5</i>	744 $\pm$ 488	1.8	0.147
<i>ITGA6</i>	684 $\pm$ 317	1.7	0.102
<i>ITGA7</i>	1 341 $\pm$ 1 476	1.1	0.881
<b><i>ITGA10</i></b>	494 $\pm$ 372	<b>-2.4</b>	0.273
<i>ITGA11</i>	494 $\pm$ 476	1.2	0.771
<i>ITGAE</i>	428 $\pm$ 303	1.4	0.375
<i>ITGAV</i>	3 978 $\pm$ 833	1.0	0.907
<i>ITGB1</i>	2 162 $\pm$ 1 117	1.1	0.863
<i>INTGB1BP1</i>	224 $\pm$ 84	1.1	0.721
<i>ITGB3</i>	196 $\pm$ 104	1.0	0.939
<i>ITGB3BP</i>	411 $\pm$ 361	1.6	0.399
<i>ITGB4</i>	933 $\pm$ 676	-1.6	0.239
<i>ITGB5</i>	6 051 $\pm$ 1 667	1.4	0.049 <sup>a</sup>
<i>ITGB7</i>	100 $\pm$ 47	1.2	0.441
<i>ITGBL1</i>	3 292 $\pm$ 1 311	-1.3	0.228

Genes with linear values under 100 were excluded. Bold indicates a twofold down- or upregulation.

<sup>a</sup>Means significantly different ( $p < 0.05$ ).



**FIG. 2.** Microarray analysis. Linear values of the microarray analysis of genes of interests. Healthy specimens (black bars) and FECD specimens (white bars).

upregulated, however, none of these deregulated genes showed statistical significance. The only deregulated genes with a *p*-value under 0.05 were the ones coding for the fibronectin type III domain containing 4 (*FNDC4*) and the integrin  $\beta$ 5 subunit (*ITGB5*) (Tables 1 and 2).

#### ECM- and integrin-related protein expression

We then examined the protein expression of these ECM and integrin-related genes, especially type IV collagen, laminin, and fibronectin, since they were previously reported to be deregulated in native FECD tissues.<sup>12,13</sup> To do so, healthy or FECD cells were seeded on a previously decellularized DM (Fig. 1A) to engineer a corneal endothelium. As shown in the histology cross sections (Fig. 1B), the engineered endothelium formed a monolayer of tightly-packed cells, similar to the native endothelium. Native tissues were used as controls for the immunostaining. A summary of the immunostaining results of ECM- and integrin-related proteins is presented in Table 3.

**TABLE 3.** SUMMARY OF EXTRACELLULAR-MATRIX-RELATED PROTEINS AND INTEGRIN SUBUNITS DETECTED BY IMMUNOFLUORESCENCE

	Native healthy	Native FECD	Engineered healthy	Engineered FECD
Extracellular matrix proteins				
Col IV	+	+ to ++	+ to ++	+ to ++
LM	+	(+)	+	+
FN	(+)	++	(+)	+ to ++
CLU	-	+	-	-
TGF $\beta$ Ip	+ <sup>a</sup>	+ <sup>a</sup>	+ <sup>a</sup>	+ <sup>a</sup>
Integrin proteins				
Int $\alpha$ 4	+	+	+	+
Int $\alpha$ 6	(+) to +	(+)	(+)	(+)
Int $\alpha$ v	(+) to +	(+)	+	+
Int $\beta$ 1	(+)	(+)	+	+

Intensity grading: ++ strong positive staining; + positive staining; (+) weak positive staining; - absence of staining.

<sup>a</sup>note that the staining was only present on the stromal side of Descemet's membrane (thus was not recently deposited by endothelial cells).

Col IV, type IV collagen; LM, laminin; FECD, Fuchs endothelial corneal dystrophy; FN, fibronectin; CLU, clusterin; TGF $\beta$ Ip, transforming growth factor  $\beta$ -induced protein; Int, integrin.

The native DM normally expresses type IV collagen as a thin line on its endothelial side (Fig. 3). A similar expression was observed in native FECD specimens, as well as in healthy and FECD-engineered endothelia (Fig. 3). Laminin protein expression was also observed in all specimens, without obvious differences between native healthy and engineered (healthy or FECD) tissues, and a weaker expression in native FECD specimens (Fig. 3). Fibronectin protein expression, on the contrary, was markedly increased in both native and engineered FECD specimens (Fig. 3).

The  $\alpha$ 4 integrin subunit was similarly expressed in all tissues (Fig. 4), while the  $\alpha$ 5 subunit was not detected in any of our samples (not shown). Integrin subunits  $\alpha$ 6 and  $\alpha$ v were present on all samples with a fainter expression in native FECD specimens. The protein expression of the integrin  $\beta$ 1 subunit was stronger in both engineered tissues (Fig. 4).

An immunostaining of the glycoprotein clusterin, known to cause cell aggregation and induce the formation of junctional contacts between cells,<sup>41</sup> was performed in combination with TGF $\beta$ Ip, an ECM protein that mediates cell adhesion by interacting with collagens, fibronectin, and integrins proteins, mainly  $\alpha$ 3 $\beta$ 1<sup>42,43</sup> (Fig. 5). In healthy and FECD native and engineered corneas, TGF $\beta$ Ip was generally expressed on the stromal side of DMs, with punctate staining also observed within DMs. Only a very faint cellular TGF $\beta$ Ip expression was observed within CECs. Clusterin was only observed in one guttae of a native FECD specimen and never in FECD-engineered corneas.

#### Discussion

This study shows that cultured FECD cells carry the disease phenotype *in vitro*. The endothelia engineered using FECD cells showed a greater deposition of fibronectin than their healthy counterpart, as early as 1–3 weeks after seeding. Fibronectin accumulation was observed without deregulation of laminin and type IV collagen, which were similarly expressed and distributed in the engineered tissues. Since laminin and type IV collagen were previously shown to be increased in late-stage FECD,<sup>12–14</sup> our results suggest that fibronectin deposition precedes deregulation of these proteins, which is compatible with the chronicity of the disease. Several decades usually separate the appearance of the first guttae and late-stage endothelial decompensation necessitating endothelial transplantation. In our model, fibronectin deposition was the earliest detected sign of FECD pathogenesis.

Our results also demonstrate a high degree of variability in gene expression among FECD specimens. This is in accordance with previous observations showing significant variation in DM phenotype in terms of membrane thickness, presence and amount of striated bodies, guttae shape, size and distribution, and presence or absence of a fibrillar layer.<sup>6,9–11,44</sup> TGF $\beta$ Ip and clusterin have previously been shown to colocalize at the guttae of FECD DM.<sup>15,16</sup> In the present study, TGF $\beta$ Ip and clusterin expression was both present in one out of three native FECD specimens, however, the two proteins did not colocalize. These results converge to suggest the existence of different subtypes of late-onset FECD, despite a similar clinical endpoint. While the sample size of this study did not lead to the identification of disease-associated genes, larger studies may, in time,

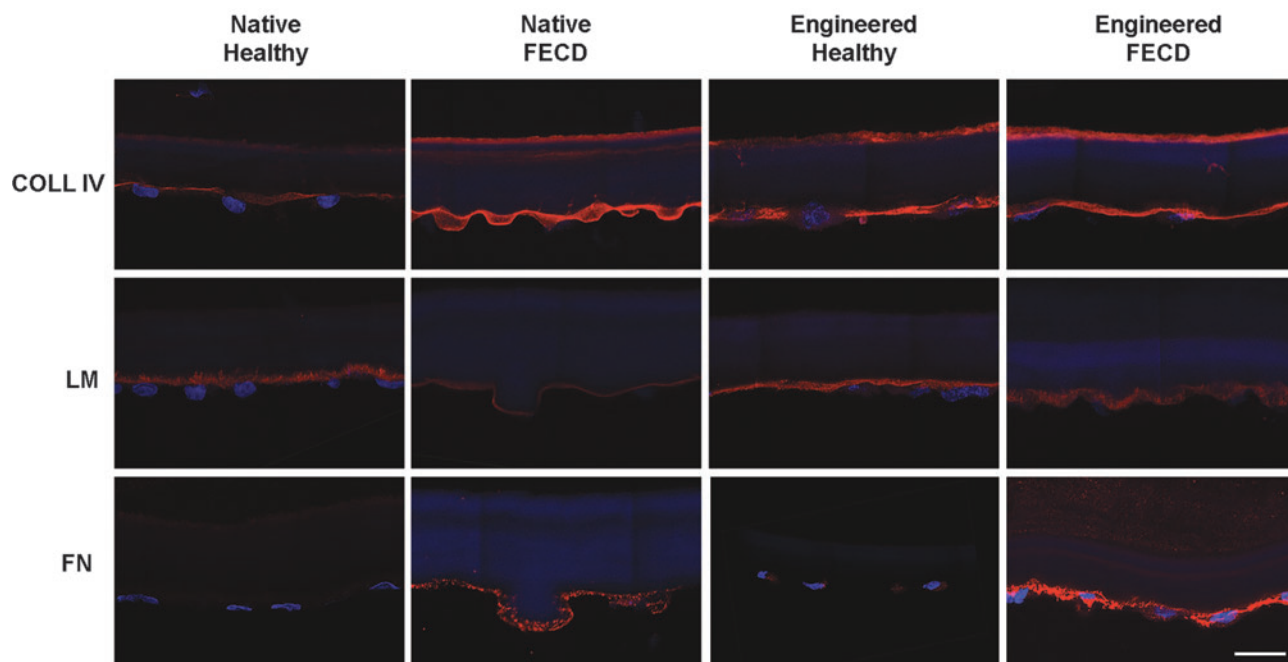


**FIG. 3.** Extracellular matrix-related protein expression. Immunofluorescent staining (*red*) of type IV collagen (COL IV), laminin (LM) and fibronectin (FN) on healthy and FECD native tissues, as well as on corneal endothelia engineered using healthy and FECD cells. Cell nuclei were counterstained with Hoechst (*blue*). Descemet membranes are oriented stromal side up and endothelial side down. Scale bar: 20  $\mu$ m.

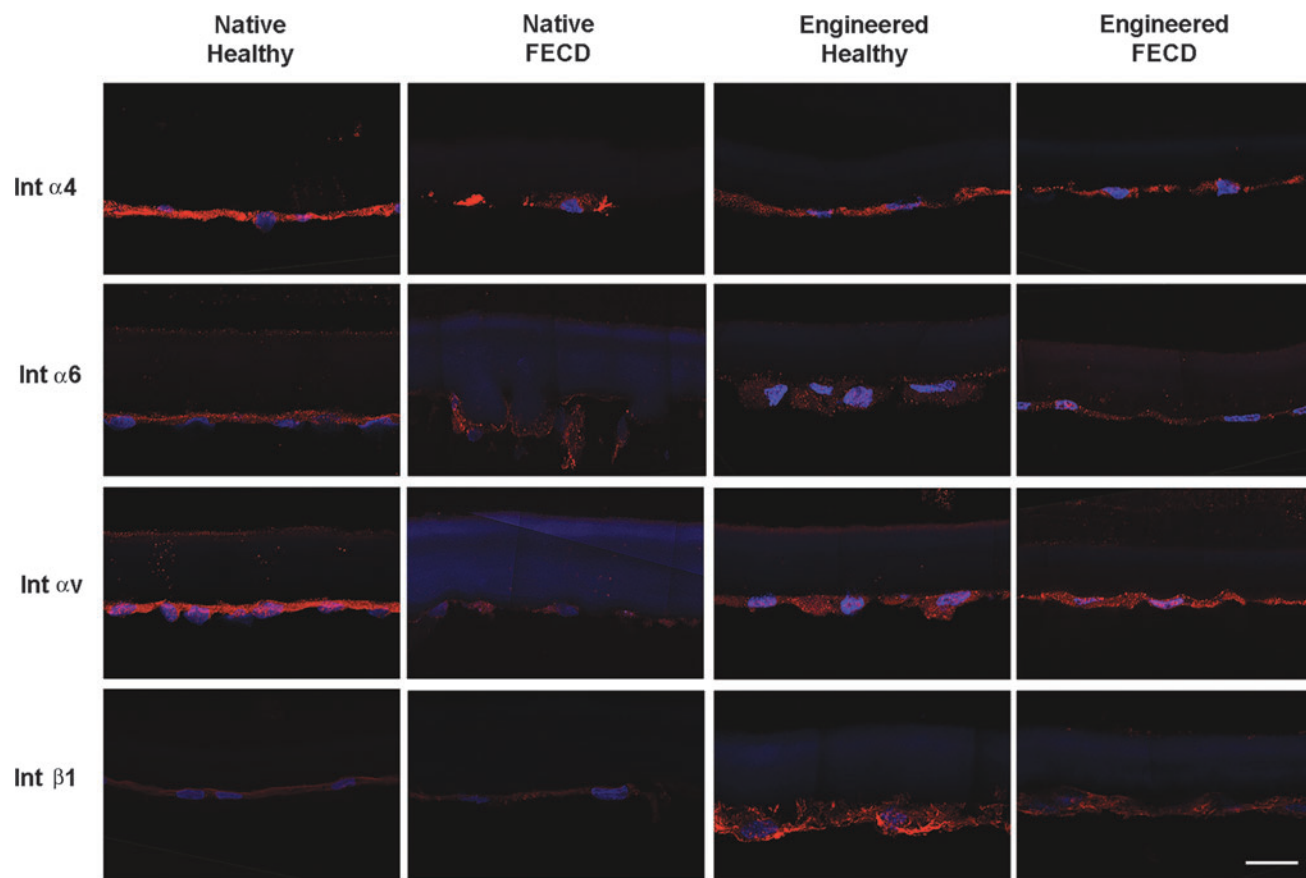


**FIG. 4.** Integrins protein expression. Immunofluorescent staining (*red*) of integrin subunits  $\alpha$ 4,  $\alpha$ 6,  $\alpha$ v, and  $\beta$ 1 on healthy and FECD native tissues, as well as on corneal endothelia engineered using healthy and FECD cells. Cell nuclei were counterstained with Hoechst (*blue*). Descemet membranes are oriented stromal side up and endothelial side down. Scale bar: 20  $\mu$ m.

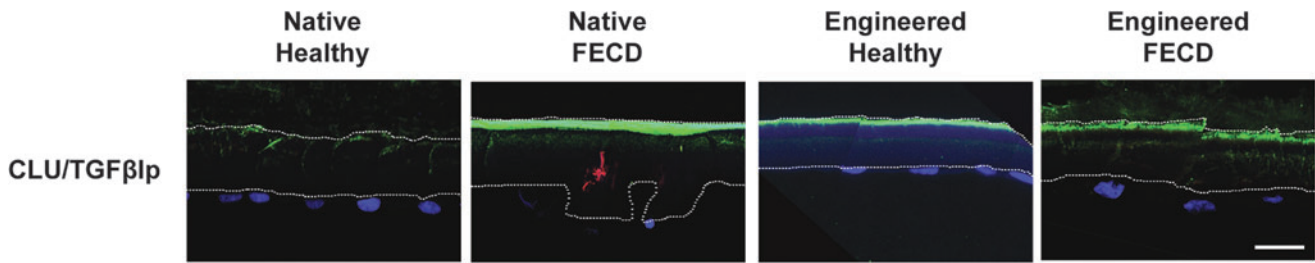


**FIG. 5.** Clusterin and TGFβ1p protein expression. Immunofluorescent staining of clusterin by (CLU; red) and TGFβ1p (green) on healthy and FECD native tissues, as well as on corneal endothelia engineered using healthy and FECD cells. Cell nuclei were counterstained with Hoechst (blue). Descemet membranes are oriented stromal side up and endothelial side down. A white line delineates Descemet membranes. Scale bar: 20 μm.

allow the separation of different FECD subtypes according to sets of deregulated genes.

The mutation L450W in the *COL8A2* gene causes an improper accumulation (between 2.3 and 5.8-fold) of the collagen type VIII α2 protein in DMs,<sup>45</sup> resulting in guttae formation and reduced endothelial cell counts.<sup>46</sup> *COL8A2* mutations (L450W and Q455V) have been identified in a rare familial early-onset subtype of FECD.<sup>12,13,47–52</sup> We did not observe an overexpression of *COL8A2* in FECD-cultured cells. One explanation is that the specimens used herein were all obtained from patients with late-onset FECD. Indeed, screening of patients with this subtype of the disease has repeatedly failed to document *COL8A2* mutations<sup>53–55</sup> or *COL8A2* gene and protein expression deregulation.<sup>14,56</sup>

The increased deposition of fibronectin by the FECD cells is in accordance with our previous experiments showing an early and enhanced deposition of ECM in a short-term living model of FECD.<sup>37</sup> Given this increased accumulation of fibronectin in FECD, it is surprising not to find any significant deregulation of the integrins binding this ECM protein (integrins α4β1, α4β7, α5β1, and αvβ3) at both the gene and the protein levels. Indeed, the integrin genes *ITGA4*, *ITGA5*, *ITGAV*, *ITGB1*, and *ITGB7*, as well as the integrin proteins α4, αv, and β1 were all similarly expressed in the cultured cells and in the endothelia engineered using healthy and FECD cells. Of interest, the integrin β5 subunit gene *ITGB5* was significantly ( $p=0.049$ ) slightly upregulated (1.4-fold) in FECD cells. The β5 integrin subunit is only known to bind with αv, and integrin αvβ5 also has fibronectin as one of its ligands.<sup>57</sup> Considering *ITGB5* was the integrin subunit with the highest linear signal, it could be meaningful to address its role in FECD pathogenesis.

The β1 integrin subunit showed a higher protein expression in the engineered endothelia compared with the native tissues (for both healthy and FECD). This suggests that cell culture, rather than the disease, is responsible for the upregulation of this integrin subunit. An upregulation of the β1 subunit could benefit the engineering of a corneal endothelium by enhancing the adhesion to a carrier or to the native DM. The endothelial side of the DM is indeed rich in laminin,<sup>3,4</sup> a protein that interacts with integrins α3β1, α6β1, and α7β1.<sup>17</sup>

Interestingly and contrary to native tissue,<sup>14</sup> very few genes and proteins were deregulated in cultured FECD cells compared with cultured healthy cells. This observation supports the hypothesis that cell culture may select the less

affected cells, allowing to engineer a functional endothelium using cells harvested from late stage FECD, as reported previously by our group.<sup>37</sup>

To conclude, our results point to an early implication of fibronectin in the pathogenesis of the disease. This increase in fibronectin seems to precede the accumulation of laminin and type IV collagen at the posterior side of DM, as well as the increase in clusterin and TGFβ1p colocalized at the guttae that have been described in the late stages of the disease. Fibronectin plays an important role in the regulation of cell migration, adhesion, growth, differentiation, and apoptosis.<sup>25</sup> Our engineered tissue model could thus be used to further study the consequence and implication of the accumulation of fibronectin and other proteins in FECD, with the hope that early pharmacological inhibition would slow down progression of the disease and eventually avoid corneal transplantation.

#### Acknowledgments

This work was supported by the “Fondation des hôpitaux HSS et HEJ” (S.P.), the Canadian Institutes of Health Research (I.B., S.P., P.J.R.) and the “Fonds de recherche du Québec–Santé” (FRQ-S) TheCell Network. Procurement of eyes and corneas for research from the CUO Eye bank was possible thanks to the FRQ-S Vision Health Research Network Infrastructure Program. I.B. is the recipient of the Charles-Albert Poissant Research Chair in Corneal Transplantation, University of Montreal, Canada. P.J.R. is a research scholar from the FRQ-S and S.P. is a research scholar from the FRQ-S in partnership with the “Fondation Antoine Turmel.” The authors thank Drs. Richard Bazin, Patricia-Ann Laughrea, and Marie-Ève Légaré from the CUO; Drs. Mona Harrissi-Dagher, Louis Racine, Paul Thompson, and Marie-Claude Robert from the CHUM and Dre Johanna Choremis from HMR for their ongoing collaboration in obtaining the FECD specimens; Myriam Bareille, Danièle Caron, Patrick Carrier, Karolyn Forget, Marie-Claude Perron, Jeanne d’Arc Uwamaliya, and the CUO de Québec and HMR-Rosemont operating room nurses for their technical assistance; Karine Zaniolo and Sylvain Guérin for the microarrays; Olivier Rochette Drouin for technical assistance and the LOEX research assistants for the histology preparations.

#### Disclosure Statement

No competing financial interests exist.

## References

1. Waring, G.O., 3rd, Bourne, W.M., Edelhauser, H.F., and Kenyon, K.R. The corneal endothelium. Normal and pathologic structure and function. *Ophthalmology* **89**, 531, 1982.
2. EBAA. 2015 Eye Banking Statistical Report. Washington D.C., 2016. <http://restoresight.org/wp-content/uploads/2016/03/2015-Statistical-Report.pdf> (accessed September 15, 2017).
3. Levy, S.G., Moss, J., Sawada, H., Dopping-Hepenstal, P.J., and McCartney, A.C. The composition of wide-spaced collagen in normal and diseased Descemet's membrane. *Curr Eye Res* **15**, 45, 1996.
4. Ljubimov, A.V., Burgeson, R.E., Butkowski, R.J., Michael, A.F., Sun, T.T., and Kenney, M.C. Human corneal basement membrane heterogeneity: topographical differences in the expression of type IV collagen and laminin isoforms. *Lab Invest* **72**, 461, 1995.
5. Johnson, D.H., Bourne, W.M., and Campbell, R.J. The ultrastructure of Descemet's membrane. I. Changes with age in normal corneas. *Arch Ophthalmol* **100**, 1942, 1982.
6. Yuen, H.K., Rassier, C.E., Jardeleza, M.S., Green, W.R., de la Cruz, Z., Stark, W.J., *et al.* A morphologic study of Fuchs dystrophy and bullous keratopathy. *Cornea* **24**, 319, 2005.
7. Naumann, G.O., and Schlotzer-Schrehardt, U. Keratopathy in pseudoexfoliation syndrome as a cause of corneal endothelial decompensation: a clinicopathologic study. *Ophthalmology* **107**, 1111, 2000.
8. Shousha, M.A., Perez, V.L., Wang, J., Ide, T., Jiao, S., Chen, Q., *et al.* Use of ultra-high-resolution optical coherence tomography to detect in vivo characteristics of Descemet's membrane in Fuchs' dystrophy. *Ophthalmology* **117**, 1220, 2010.
9. Iwamoto, T., and DeVoe, A.G. Electron microscopic studies on Fuchs' combined dystrophy. I. Posterior portion of the cornea. *Invest Ophthalmol* **10**, 9, 1971.
10. Bourne, W.M., Johnson, D.H., and Campbell, R.J. The ultrastructure of Descemet's membrane. III. Fuchs' dystrophy. *Arch Ophthalmol* **100**, 1952, 1982.
11. Zaniolo, K., Bostan, C., Rochette Drouin, O., Deschambeault, A., Perron, M.C., Brunette, I., *et al.* Culture of human corneal endothelial cells isolated from corneas with Fuchs endothelial corneal dystrophy. *Exp Eye Res* **94**, 22, 2012.
12. Gottsch, J.D., Zhang, C., Sundin, O.H., Bell, W.R., Stark, W.J., and Green, W.R. Fuchs corneal dystrophy: aberrant collagen distribution in an L450 W mutant of the COL8A2 gene. *Invest Ophthalmol Vis Sci* **46**, 4504, 2005.
13. Zhang, C., Bell, W.R., Sundin, O.H., De La Cruz, Z., Stark, W.J., Green, W.R., *et al.* Immunohistochemistry and electron microscopy of early-onset fuchs corneal dystrophy in three cases with the same L450W COL8A2 mutation. *Trans Am Ophthalmol Soc* **104**, 85, 2006.
14. Weller, J.M., Zenkel, M., Schlotzer-Schrehardt, U., Bachmann, B.O., Tourtas, T., and Kruse, F.E. Extracellular matrix alterations in late-onset Fuchs' corneal dystrophy. *Invest Ophthalmol Vis Sci* **55**, 3700, 2014.
15. Jurkunas, U.V., Bitar, M., and Rawe, I. Colocalization of increased transforming growth factor-beta-induced protein (TGFB $\beta$ ) and Clusterin in Fuchs endothelial corneal dystrophy. *Invest Ophthalmol Vis Sci* **50**, 1129, 2009.
16. Jurkunas, U.V., Bitar, M.S., Rawe, I., Harris, D.L., Colby, K., and Joyce, N.C. Increased clusterin expression in Fuchs' endothelial dystrophy. *Invest Ophthalmol Vis Sci* **49**, 2946, 2008.
17. Hynes, R.O. Integrins: bidirectional, allosteric signaling machines. *Cell* **110**, 673, 2002.
18. Vigneault, F., Zaniolo, K., Gaudreault, M., Gingras, M.E., and Guerin, S.L. Control of integrin genes expression in the eye. *Prog Retin Eye Res* **26**, 99, 2007.
19. Takada, Y., Ye, X., and Simon, S. The integrins. *Genome Biol* **8**, 215, 2007.
20. Elner, S.G., and Elner, V.M. The integrin superfamily and the eye. *Invest Ophthalmol Vis Sci* **37**, 696, 1996.
21. Legate, K.R., and Fassler, R. Mechanisms that regulate adaptor binding to beta-integrin cytoplasmic tails. *J Cell Sci* **122**, 187, 2009.
22. Wiesner, S., Legate, K.R., and Fassler, R. Integrin-actin interactions. *Cell Mol Life Sci* **62**, 1081, 2005.
23. Shattil, S.J., Kim, C., and Ginsberg, M.H. The final steps of integrin activation: the end game. *Nat Rev Mol Cell Biol* **11**, 288, 2010.
24. Cordes, N., and Park, C.C. beta1 integrin as a molecular therapeutic target. *Int J Radiat Biol* **83**, 753, 2007.
25. Aota, S., and Yamada, K.M. Fibronectin and cell adhesion: specificity of integrin-ligand interaction. *Adv Enzymol Relat Areas Mol Biol* **70**, 1, 1995.
26. Wehrle-Haller, B., and Imhof, B.A. Integrin-dependent pathologies. *J Pathol* **200**, 481, 2003.
27. Lowell, C.A., and Mayadas, T.N. Overview: studying integrins in vivo. *Methods Mol Biol* **757**, 369, 2012.
28. Choi, J.S., Kim, E.Y., Kim, M.J., Giegengack, M., Khan, F.A., Khang, G., *et al.* In vitro evaluation of the interactions between human corneal endothelial cells and extracellular matrix proteins. *Biomed Mater* **8**, 014108, 2013.
29. Kenney, M.C., Labermeier, U., Hinds, D., and Waring, G.O., 3rd. Characterization of the Descemet's membrane/posterior collagenous layer isolated from Fuchs' endothelial dystrophy corneas. *Exp Eye Res* **39**, 267, 1984.
30. Borderie, V.M., Baudrimont, M., Vallee, A., Ereau, T.L., Gray, F., and Laroche, L. Corneal endothelial cell apoptosis in patients with Fuchs' dystrophy. *Invest Ophthalmol Vis Sci* **41**, 2501, 2000.
31. Gottsch, J.D., Seitzman, G.D., Margulies, E.H., Bowers, A.L., Michels, A.J., Saha, S., *et al.* Gene expression in donor corneal endothelium. *Arch Ophthalmol* **121**, 252, 2003.
32. Elhali, H., Azizi, B., and Jurkunas, U.V. Fuchs endothelial corneal dystrophy. *Ocul Surf* **8**, 173, 2010.
33. Proulx, S., Bourget, J.M., Gagnon, N., Martel, S., Deschambeault, A., Carrier, P., *et al.* Optimization of culture conditions for porcine corneal endothelial cells. *Mol Vis* **13**, 524, 2007.
34. Proulx, S., d'Arc Uwamaliya, J., Carrier, P., Deschambeault, A., Audet, C., Giasson, C.J., *et al.* Reconstruction of a human cornea by the self-assembly approach of tissue engineering using the three native cell types. *Mol Vis* **16**, 2192, 2010.
35. Proulx, S., Bensaoula, T., Nada, O., Audet, C., d'Arc Uwamaliya, J., Devaux, A., *et al.* Transplantation of a tissue-engineered corneal endothelium reconstructed on a devitalized carrier in the feline model. *Invest Ophthalmol Vis Sci* **50**, 2686, 2009.
36. Proulx, S., Audet, C., Uwamaliya, J., Deschambeault, A., Carrier, P., Giasson, C.J., *et al.* Tissue engineering of feline corneal endothelium using a devitalized human cornea as carrier. *Tissue Eng Part A* **15**, 1709, 2009.
37. Haydari, M.N., Perron, M.C., Laprise, S., Roy, O., Cameron, J.D., Proulx, S., *et al.* A short-term in vivo experimental model for Fuchs endothelial corneal dystrophy. *Invest Ophthalmol Vis Sci* **53**, 6343, 2012.
38. Joyce, N.C., and Zhu, C.C. Human corneal endothelial cell proliferation: potential for use in regenerative medicine. *Cornea* **23**, S8, 2004.



39. Gendron, S.P., Theriault, M., Proulx, S., Brunette, I., and Rochette, P.J. Restoration of mitochondrial integrity, telomere length, and sensitivity to oxidation by in vitro culture of Fuchs' endothelial corneal dystrophy cells. *Invest Ophthalmol Vis Sci* **57**, 5926, 2016.
40. Brazma, A., Hingamp, P., Quackenbush, J., Sherlock, G., Spellman, P., Stoeckert, C., *et al.* Minimum information about a microarray experiment (MIAME)-toward standards for microarray data. *Nat Genet* **29**, 365, 2001.
41. Schwochau, G.B., Nath, K.A., and Rosenberg, M.E. Clusterin protects against oxidative stress in vitro through aggregative and nonaggregative properties. *Kidney Int* **53**, 1647, 1998.
42. Runager, K., Enghild, J.J., and Klintworth, G.K. Focus on molecules: transforming growth factor beta induced protein (TGFBIp). *Exp Eye Res* **87**, 298, 2008.
43. Billings, P.C., Whitbeck, J.C., Adams, C.S., Abrams, W.R., Cohen, A.J., Engelsberg, B.N., *et al.* The transforming growth factor-beta-inducible matrix protein (beta)ig-h3 interacts with fibronectin. *J Biol Chem* **277**, 28003, 2002.
44. Bergmanson, J.P., Sheldon, T.M., and Goosey, J.D. Fuchs' endothelial dystrophy: a fresh look at an aging disease. *Ophthalmic Physiol Opt* **19**, 210, 1999.
45. Kelliher, C., Chakravarti, S., Vij, N., Mazur, S., Stahl, P.J., Engler, C., *et al.* A cellular model for the investigation of Fuchs' endothelial corneal dystrophy. *Exp Eye Res* **93**, 880, 2011.
46. Matthaei, M., Hu, J., Meng, H., Lackner, E.M., Eberhart, C.G., Qian, J., *et al.* Endothelial cell whole genome expression analysis in a mouse model of early-onset Fuchs' endothelial corneal dystrophy. *Invest Ophthalmol Vis Sci* **54**, 1931, 2013.
47. Biswas, S., Munier, F.L., Yardley, J., Hart-Holden, N., Perveen, R., Cousin, P., *et al.* Missense mutations in COL8A2, the gene encoding the alpha2 chain of type VIII collagen, cause two forms of corneal endothelial dystrophy. *Hum Mol Genet* **10**, 2415, 2001.
48. Kobayashi, A., Fujiki, K., Murakami, A., Kato, T., Chen, L.Z., Onoe, H., *et al.* Analysis of COL8A2 gene mutation in Japanese patients with Fuchs' endothelial dystrophy and posterior polymorphous dystrophy. *Jpn J Ophthalmol* **48**, 195, 2004.
49. Gottsch, J.D., Sundin, O.H., Liu, S.H., Jun, A.S., Broman, K.W., Stark, W.J., *et al.* Inheritance of a novel COL8A2 mutation defines a distinct early-onset subtype of fuchs corneal dystrophy. *Invest Ophthalmol Vis Sci* **46**, 1934, 2005.
50. Liskova, P., Prescott, Q., Bhattacharya, S.S., and Tuft, S.J. British family with early-onset Fuchs' endothelial corneal dystrophy associated with p.L450W mutation in the COL8A2 gene. *Br J Ophthalmol* **91**, 1717, 2007.
51. Mok, J.W., Kim, H.S., and Joo, C.K. Q455V mutation in COL8A2 is associated with Fuchs' corneal dystrophy in Korean patients. *Eye (Lond)* **23**, 895, 2009.
52. Minear, M.A., Li, Y.J., Rimmler, J., Balajonda, E., Watson, S., Allingham, R.R., *et al.* Genetic screen of African Americans with Fuchs endothelial corneal dystrophy. *Mol Vis* **19**, 2508, 2013.
53. Afshari, N.A., Li, Y.J., Pericak-Vance, M.A., Gregory, S., and Klintworth, G.K. Genome-wide linkage scan in Fuchs endothelial corneal dystrophy. *Invest Ophthalmol Vis Sci* **50**, 1093, 2009.
54. Hemadevi, B., Srinivasan, M., Arunkumar, J., Prajna, N.V., and Sundaresan, P. Genetic analysis of patients with Fuchs endothelial corneal dystrophy in India. *BMC Ophthalmol* **10**, 3, 2010.
55. Kuot, A., Hewitt, A.W., Griggs, K., Klebe, S., Mills, R., Jhanji, V., *et al.* Association of TCF4 and CLU polymorphisms with Fuchs' endothelial dystrophy and implication of CLU and TGFBI proteins in the disease process. *Eur J Hum Genet* **20**, 632, 2012.
56. Poulsen, E.T., Dyrland, T.F., Runager, K., Scavenius, C., Krogager, T.P., Hojrup, P., *et al.* Proteomics of Fuchs' endothelial corneal dystrophy support that the extracellular matrix of Descemet's membrane is disordered. *J Proteome Res* **13**, 4659, 2014.
57. Chen, J., Maeda, T., Sekiguchi, K., and Sheppard, D. Distinct structural requirements for interaction of the integrins alpha 5 beta 1, alpha v beta 5, and alpha v beta 6 with the central cell binding domain in fibronectin. *Cell Adhes Commun* **4**, 237, 1996.

Address correspondence to:

*Stéphanie Proulx, PhD*

*Centre de Recherche du CHU de Québec-Université Laval*

*Axe Médecine Régénératrice*

*Hôpital du Saint-Sacrement*

*1050 chemin Sainte-Foy*

*Québec G1S 4L8*

*QC*

*Canada*

*E-mail: stephanie.proulx@fmed.ulaval.ca*

*Received: March 16, 2017*

*Accepted: July 14, 2017*

*Online Publication Date: September 28, 2017*